Linear-response theory of Coulomb drag in coupled electron systems

Karsten Flensberg,* Ben Yu-Kuang Hu, and Antti-Pekka Jauho
Mikroelektronik Centret, Danmarks Tekniske Universitet, DK-2800 Lyngby, Denmark

Jari M. Kinaret†
Nordita, Blegdamsvej 17, DK-2100 København Ø, Denmark
(Received 21 April 1995)

We report a fully microscopic theory for the transconductivity, or, equivalently, the momentum transfer rate, of Coulomb coupled electron systems. We use the Kubo linear-response formalism and our main formal result expresses the transconductivity in terms of two fluctuation diagrams, which are topologically related but not equivalent to the Aslamazov-Larkin diagrams known from superconductivity. Results reported elsewhere are shown to be special cases of our general expression; specifically, we recover the Boltzmann equation result in the semiclassical clean limit and the memory function results for dirty systems with constant impurity scattering rates. Furthermore, we show that for energy-dependent relaxation times, the final result is not expressible in terms of standard density-response functions. Other results include (i) at $T = 0$, the frequency dependence of the transfer rate is found to be proportional to Ω and Ω^2 for frequencies below and above the impurity scattering rate, respectively, and (ii) the weak localization correction to the transconductivity is given by $\delta\sigma_{21}^{\mathrm{WL}} \propto \delta\sigma_{11}^{\mathrm{WL}} + \delta\sigma_{22}^{\mathrm{WL}}$.

I. INTRODUCTION

Consider two systems containing mobile charge carriers so close to each other that the charges in the two respective subsystems experience the Coulomb forces originating from the other subsystem and yet far enough away from each other that direct charge transfer between the two subsystems is not possible. Experimental realizations of such systems are, for example, Coulomb coupled double-quantum-well systems,[1,2] arrangements where a three-dimensional system is close to a two-dimensional system,[3] or two nearby quantum wires. A scattering event between a carrier in the system and a carrier in another system leads to momentum transfer between the two subsystems. Thus, if a current is driven through one of the systems (henceforth the driven system is denoted as layer 1), then an induced current is dragged in the other subsystem (layer 2). Alternatively, if no current is allowed to flow in layer 2, a voltage is induced. Due to momentum conservation the two particle number currents flow in the same direction. Since the mechanism for the Coulomb drag is carrier-carrier scattering the drag current is proportional to the square of the effective interaction between the subsystems. The available phase space for electron-electron scattering tends to zero at low temperatures and consequently one expects Coulomb drag to decrease with decreasing temperature. At low temperatures, the two Pauli factors entering the carrier-carrier scattering rate lead to a T^2 dependence and this behavior is approximately seen in experiments.[1] Note, however, that there are small but important deviations from the simple T^2 law; these deviations have been the topic of much recent interest.[1,4,5]

The possibility for Coulomb drag was realized already long ago[6,7] and the recent experimental advances[1–3] have brought about a flurry of theoretical works. A number of different theoretical approaches have been proposed. These include (i) calculations based on the Boltzmann equation,[1,8] (ii) the memory function approach of Ref. 9, and (iii) the momentum balance equation method.[4]

In this paper, we calculate the Coulomb drag between two systems using a fully microscopic theory based on a linear-response formula. The central object to be evaluated is the retarded current-current correlation function; since the two currents involved refer to the the two different subsystems, we call the result of this calculation *transconductivity*. The motivation underlying our work is that all previously proposed approaches lack the rigor that can be achieved with a formal linear-response calculation. The present method allows us to identify the Feynman diagrams that contribute to the transconductivity. Instead of the normal conductivity bubble, we find that one must evaluate a fluctuation diagram, which is similar but not identical to the Aslamazov-Larkin[10] diagrams known from superconductivity or the diagrams encountered in connection with the microscopic theory of van der Waals interactions.[11,12] Thus all the methods developed within the diagrammatic perturbation theory are readily applicable and one can systematically study the effects of higher-order-scattering processes, such as vertex corrections or weak localization, electron-phonon interactions, or the effect of magnetic fields.

Apart from the general formulation for calculating transconductivities, we obtain the following explicit results. In the limit of weak impurity scattering we show that the linear-response result reduces to the expression obtained with the Boltzmann equation. In this limit, for energy-*independent* scattering times, this result de-

0163-1829/95/52(20)/14761(14)/$06.00

pends on the susceptibility functions of the individual subsystems, as obtained in previous works,[1,8] whereas for energy-*dependent* scattering times, the susceptibility functions must be generalized, as shown by two of us utilizing the Boltzmann equation.[13]

We also study the corrections to the Boltzmann equation formula in the case of stronger impurity scattering, i.e., accounting for vertex corrections. We also consider weak localization corrections to the transconductivity. All these effects are calculated at finite temperature, but for zero external frequency. At $T = 0$ finite frequency calculations become feasible and we present a general proof that the drag current vanishes in the dc limit at zero temperature for an *open* system. Recently, Rojo and Mahan[14] used a ground-state energy argument to calculate the drag current and found a nonzero result at zero temperature. This seems to contradict our results; however, there is an important distinction: the calculation of Ref. 14 applies for *closed* systems, e.g., coupled mesoscopic rings.

This paper is organized as follows. Section II outlines the derivation of the general expression for transconductivity. Section III is devoted to impurity scattering: first, we show how the well-known Boltzmann result follows from the general formulation and then, we establish a connection to the memory function formulation of Ref. 9. This section concludes with a discussion of energy-dependent scattering rates and weak localization effects. Section IV presents result for $T = 0$ at finite frequency. Finally, a number of technical details can be found in the Appendixes.

II. GENERAL FORMULA FOR THE TRANSCONDUCTIVITY

The previous works have related Coulomb drag to the *transresistivity* ρ_{21}; our calculation, which is based on a Kubo formula, leads to the *transconductivity* σ_{21}. These are defined as

$$\rho_{21} = \frac{E_2}{J_1} \quad \text{with } J_2 = 0, \tag{1a}$$

$$\sigma_{21} = \frac{J_2}{E_1} \quad \text{with } E_2 = 0, \tag{1b}$$

where E_i and J_i are, respectively, the electric field and the current density in layer i. These two quantities are related via

$$\rho_{21} = \frac{-\sigma_{21}}{\sigma_{11}\sigma_{22} - \sigma_{12}\sigma_{21}} \approx \frac{-\sigma_{21}}{\sigma_{11}\sigma_{22}} . \tag{2}$$

In (2) the diagonal σ's are the individual subsystem conductivities and we note that the transconductivity is always much smaller than intralayer conductivity, because it is caused by a screened interaction between spatially separated systems (e.g., the data of Ref. 1 give $\sigma_{21}/\sigma_{11} \simeq 10^{-6}$). The transresistivity ρ_{21} is a more physically relevant quantity than σ_{21} in a drag-rate measurement because ρ_{21} is directly related to the rate of momentum transfer from particles in layer 1 to layer 2, τ_{21}^{-1}, without reference to the scattering rates of the individual layers, i.e.,

$$\rho_{21} = \frac{m_1}{n_1 e^2 \tau_{21}}, \qquad \frac{1}{\tau_{21}} = \frac{\overline{(\partial p_2/\partial t)_{\rm drag}}}{\overline{p}_1}, \tag{3}$$

where m is the effective mass, n is the carrier density, p is the momentum per particle, $(\partial p/\partial t)_{\rm drag}$ is the momentum transfer due to interlayer interactions, and the overline denotes an ensemble average.

The Kubo formula[15] expresses the conductivity tensor in terms of the retarded current-current correlation function

$$\sigma_{ij}^{\alpha\beta}(\boldsymbol{x}-\boldsymbol{x}';\Omega) = \frac{ie^2}{\Omega}\Pi_{ij}^{\alpha\beta,r}(\boldsymbol{x}-\boldsymbol{x}';\Omega) + \frac{ie^2}{m\Omega}\delta(\boldsymbol{x}-\boldsymbol{x}')\delta_{ij}\delta_{\alpha\beta}\rho_i(\boldsymbol{x}), \tag{4}$$

where (throughout we use $\hbar = 1$)

$$\Pi_{ij}^{\alpha\beta,r}(\boldsymbol{x}-\boldsymbol{x}';t-t') = -i\Theta(t-t')\langle[j_i^\alpha(\boldsymbol{x},t), j_j^\beta(\boldsymbol{x}',t')]\rangle. \tag{5}$$

Here $\{ij\}$ indicate the subsystem, $\{\alpha\beta\}$ in the superscripts label the Cartesian coordinates, $\rho_i(\boldsymbol{x})$ is the particle density in subsystem i, and $\boldsymbol{j}(\boldsymbol{x},t)$ is the particle current operator. We have assumed that the subsystems are translationally invariant. Our task consists of calculating the transconductivity $\sigma_{21}^{\alpha\beta}$.

We employ the imaginary-time formalism to evaluate the retarded current-current correlation function, starting with the (imaginary-)time-ordered correlation function

$$\Pi_{21}^{\alpha\beta}(\boldsymbol{x}-\boldsymbol{x}';\tau-\tau') = -\langle T_\tau\{j_1^\alpha(\boldsymbol{x},\tau)j_2^\beta(\boldsymbol{x}',\tau')\}\rangle. \tag{6}$$

The retarded function then follows as

$$\Pi_{21}^{\alpha\beta,r}(\boldsymbol{x}-\boldsymbol{x}';\Omega) = \lim_{i\Omega_n\to\Omega+i\delta}\Pi_{21}^{\alpha\beta}(\boldsymbol{x}-\boldsymbol{x}';i\Omega_n), \tag{7}$$

where

$$\Pi_{21}^{\alpha\beta}(\boldsymbol{x}-\boldsymbol{x}';i\Omega_n) = \int_0^\beta d\tau\, e^{i\Omega_n\tau}\Pi_{21}^{\alpha\beta}(\boldsymbol{x}-\boldsymbol{x}';\tau)\ , \tag{8}$$

$$\Pi_{21}^{\alpha\beta}(\boldsymbol{x}-\boldsymbol{x}';\tau) = \frac{1}{\beta}\sum_n e^{-i\Omega_n\tau}\Pi_{21}^{\alpha\beta}(\boldsymbol{x}-\boldsymbol{x}';i\Omega_n), \tag{9}$$

and $\beta = 1/k_BT$. The calculation proceeds by expanding the transconductivity in powers of the interaction between the subsystems. The interaction Hamiltonian is given by

$$H_{12} = \int d\boldsymbol{r_1}\int d\boldsymbol{r_2}\ \rho_1(\boldsymbol{r_1})\,U_{12}(\boldsymbol{r_1}-\boldsymbol{r_2})\,\rho_2(\boldsymbol{r_2}). \tag{10}$$

Here U_{12} is the bare Coulomb interaction between the systems. We note that other interaction processes, which couple the charge carriers in the two subsystems, can be treated similarly. An important example is the virtual-phonon-mediated interaction, which may play a role in

the low-temperature behavior of the momentum transfer rate.[1,4]

The τ dependence of the current operators in (5) is determined by the full Hamiltonian $H = H_1 + H_2 + H_{12}$, where H_i are the subsystem Hamiltonians. In order to develop a perturbation expansion, we must isolate the H_{12} dependence. Following the standard many-body prescription,[15] we transform into the interaction representation and obtain

$$\Pi_{21}^{\alpha\beta}(\boldsymbol{x}-\boldsymbol{x}',\tau-\tau') = -\frac{\langle T_\tau\{S(\beta)\hat{j}_1^\alpha(\boldsymbol{x},\tau)\hat{j}_2^\beta(\boldsymbol{x}',\tau')\}\rangle}{\langle S(\beta)\rangle}, \tag{11}$$

where the carets indicate that the time dependence is now governed by the individual subsystem Hamiltonians and the operator $S(\beta)$ is

$$S(\beta) = T_\tau\left\{\exp\left[-\int_0^\beta d\tau_1 \hat{H}_{12}(\tau_1)\right]\right\}. \tag{12}$$

As usual, only connected diagrams need to be included. It is now straightforward to expand $S(\beta)$ in powers of $\hat{H}_{12}$,

$$S(\beta) \approx 1 - T_\tau\left\{\int_0^\beta d\tau_1 \hat{H}_{12}(\tau_1)\right\} + \frac{1}{2}T_\tau\left\{\int_0^\beta d\tau_1 \int_0^\beta d\tau_2 \hat{H}_{12}(\tau_1)\hat{H}_{12}(\tau_2)\right\} + \cdots . \tag{13}$$

The zeroth-order term leads to a vanishing contribution to the transconductivity because the two current operators are decoupled and hence commute. In the following sections we discuss the higher-order terms.

A. Linear expansion

The linear-order term in H_{12} leads to the correlation function

$$\Pi_{21}^{\alpha\beta}(\boldsymbol{x}-\boldsymbol{x}',\tau-\tau')^{(1)} = \int_0^\beta d\tau_1 \int d\boldsymbol{r_1} d\boldsymbol{r_2} \langle T_\tau\{\hat{j}_1^\alpha(\boldsymbol{x},\tau)\hat{\rho}_1(\boldsymbol{r_1},\tau_1)\}\rangle \times U_{12}(\boldsymbol{r_1}-\boldsymbol{r_2})\langle T_\tau\{\hat{\rho}_2(\boldsymbol{r_2},\tau_1)\hat{j}_2^\beta(\boldsymbol{x}',\tau')\}\rangle. \tag{14}$$

Use of the continuity equation $i\Omega\rho + \nabla\cdot\boldsymbol{j} = 0$ allows us to eliminate the number density operator and to express the density-current correlators in terms of the subsystem conductivities. After some simplification we find (for a translationally invariant impurity averaged system where impurity scattering in the two subsystems is uncorrelated[16])

$$\sigma_{21}^{\alpha\beta}(\boldsymbol{q},\Omega)^{(1)} = \frac{1}{ie^2\Omega}\sum_{\gamma,\delta}\sigma_{22}^{\alpha\gamma}(\boldsymbol{q},\Omega)\,q^\gamma\,U_{12}(\boldsymbol{q})\,q^\delta\,\sigma_{11}^{\delta\beta}(\boldsymbol{q},\Omega). \tag{15}$$

This expression is exact and it can be used to calculate the first-order transconductivity for any system, once the subsystem conductivities σ_{ii} are known.[17] From (15) we also infer that the first-order transconductivity vanishes in the dc limit.

B. Quadratic expansion

To evaluate $\Pi_{21}^{\alpha\beta}$ to second order in H_{12}, we substitute the third term of (13) on the right-hand side of (11) and find that the current-current correlation function is given by

$$\Pi_{21}^{\alpha\beta}(\boldsymbol{x}-\boldsymbol{x}';\tau-\tau')^{(2)} = -\frac{1}{2}\int_0^\beta d\tau_1 \int_0^\beta d\tau_2 \int d\boldsymbol{r}_1 \int d\boldsymbol{r}_2 \int d\boldsymbol{r}_1' \int d\boldsymbol{r}_2' \times U_{12}(\boldsymbol{r}_1-\boldsymbol{r}_2)U_{12}(\boldsymbol{r}_1'-\boldsymbol{r}_2') \times \Delta_1^\alpha(\boldsymbol{x}\tau,\boldsymbol{r}_1\tau_1,\boldsymbol{r}_1'\tau_2)\Delta_2^\beta(\boldsymbol{x}'\tau',\boldsymbol{r}_2\tau_1,\boldsymbol{r}_2'\tau_2), \tag{16}$$

where we have defined the function

$$\Delta_i^\alpha(\boldsymbol{x}\tau,\boldsymbol{x}'\tau',\boldsymbol{x}''\tau'') = -\langle T_\tau\{\hat{j}_i^\alpha(\boldsymbol{x}\tau)\hat{\rho}_i(\boldsymbol{x}'\tau')\hat{\rho}_i(\boldsymbol{x}''\tau'')\}\rangle. \tag{17}$$

Just as in the preceding subsection, we factorized the time-ordered expectation value involving two current and four density operators; this step is justified because the two subsystems are decoupled after the formal expansion in H_{12}. Due to the assumed translational invariance Δ depends on only two coordinate differences. We define the Fourier transform $\Delta(\boldsymbol{q},\boldsymbol{q}';\omega,\omega')$ via (ν = the volume)

$$\Delta(\boldsymbol{x}\tau,\boldsymbol{x}'\tau',\boldsymbol{x}''\tau'') = \frac{1}{\nu^2}\sum_{\boldsymbol{q}_1,\boldsymbol{q}_2}\frac{1}{\beta^2}\sum_{i\omega_m,i\omega_n} \times e^{i\boldsymbol{q}_1\cdot(\boldsymbol{x}-\boldsymbol{x}'')+i\boldsymbol{q}_2\cdot(\boldsymbol{x}'-\boldsymbol{x}'')}e^{-i\omega_m(\tau-\tau'')-i\omega_n(\tau'-\tau'')} \times\Delta(\boldsymbol{q}_1+\boldsymbol{q}_2,\boldsymbol{q}_2;i\omega_m+i\omega_n,i\omega_n). \tag{18}$$

The final expression for $\Pi_{21}^{\alpha\beta}(\boldsymbol{Q},i\Omega_n)^{(2)}$ then takes the form

$$\Pi_{21}^{\alpha\beta}(\boldsymbol{Q};i\Omega_n)^{(2)} = -\frac{1}{2}\frac{1}{\nu}\sum_{\boldsymbol{q}}\frac{1}{\beta}\sum_{i\omega_n}U_{12}(\boldsymbol{q})U_{12}^*(\boldsymbol{Q}+\boldsymbol{q}) \times\Delta_1^\alpha(\boldsymbol{Q}+\boldsymbol{q},\boldsymbol{q};i\Omega_n+i\omega_n,i\omega_n) \times\Delta_2^\beta(-\boldsymbol{Q}-\boldsymbol{q},-\boldsymbol{q};-i\Omega_n-i\omega_n,-i\omega_n). \tag{19}$$

The diagram corresponding to the second-order result Eq. (19) is shown in Fig. 1. We also display the first-order term discussed above.

Consider next the $i\omega_n$ summations. The function $\Delta(z+i\Omega_n,z)$ has branch cuts in the complex z plane at $\mathrm{Im}(i\Omega_n+z)=0$ or $\mathrm{Im}(z)=0$ and is analytic elsewhere (see Appendix A). We can therefore perform the $i\omega_n$ sum as a contour integral. When we extract the retarded part

according to Eq. (7), we obtain the result

$$S(\Omega) \equiv \frac{1}{\beta}\sum_{i\omega_n} \Delta_1(i\Omega_n + i\omega_n, i\omega_n) \times \Delta_2(-i\Omega_n - i\omega_n, -i\omega_n)|_{i\Omega_n \to \Omega + i\delta} \equiv S_1(\Omega) + S_2(\Omega), \tag{20a}$$

$$S_1(\Omega) = P\int_{-\infty}^{\infty} \frac{d\omega}{2\pi i}\,[n_B(\omega+\Omega) - n_B(\omega)] \times \Delta_1(+,-)\Delta_2(-,+)\ , \tag{20b}$$

$$S_2(\Omega) = P\int_{-\infty}^{\infty} \frac{d\omega}{2\pi i}[n_B(\omega)\Delta_1(+,+)\Delta_2(-,-) - n_B(\omega+\Omega)\Delta_1(-,-)\Delta_2(+,+)], \tag{20c}$$

where $n_B(\omega)$ is the Bose function. We have suppressed the Cartesian indices and the momentum labels, since they can be gleaned from Eq. (19), and have used the notation

$$\Delta_1(\pm,\pm) = \Delta(i\Omega_n + i\omega_n \to \Omega + \omega \pm i\delta;\ i\omega_n \to \omega \pm i\delta), \tag{21a}$$

$$\Delta_2(\pm,\pm) = \Delta(-i\Omega_n - i\omega_n \to -\Omega - \omega \pm i\delta \quad -i\omega_n \to -\omega \pm i\delta)\ . \tag{21b}$$

The functions $\Delta_i(+,+)$ and $\Delta_i(-,-)$ vanish identically in the dc limit, which is proven in Appendix B.

Consider next the dc response $\Omega \to 0$ of a uniform system ($\boldsymbol{Q} = 0$). The dc limit of $S_1(\Omega)$ is simple to evaluate because the difference of the two Bose functions combined the prefactor Ω^{-1} just gives $\partial_\omega n_B(\omega)$. Thus the dc transconductivity reduces to (reintroducing $\hbar$)

$$\sigma_{21}^{\alpha\beta(2)} = \frac{e^2}{\hbar}\left(-\frac{1}{2}\right)\frac{1}{\nu}\sum_{\boldsymbol{q}}\int_{-\infty}^{\infty}\frac{d\omega}{2\pi}\,|U_{12}(\boldsymbol{q})|^2\,[\partial_\omega n_B(\omega)] \times \Delta_1^{\alpha}(\boldsymbol{q},\boldsymbol{q};\omega+i\delta,\omega-i\delta) \times \Delta_2^{\beta}(-\boldsymbol{q},-\boldsymbol{q};-\omega-i\delta,-\omega+i\delta)\ . \tag{22}$$

The actual evaluation of this expression at various levels of approximation forms the main task of this paper. In the case of electron-hole systems the overall sign of (22) must be changed.

C. Higher-order terms

The S-matrix expansion (13) can be used to generate higher-order terms. To proceed systematically one must apply the techniques of the many-body formalism. As usual, the most important processes should be identified and the corresponding diagrams be summed to infinite order. This procedure may then lead to an integral equation for the effective interaction, e.g., in the ladder approximation one obtains the Bethe-Salpeter equation. We do not pursue this line of argument further in this paper, but note that a particularly useful resummation can be obtained, if one includes the "bubble" diagrams (see Fig. 2), which leads to an effective screened interaction $V_{12}(q,\omega) = U_{12}(q)/\epsilon_{12}(q,\omega)$, where the dielectric function is given by

$$\epsilon_{12}(q,\omega) = [1 - U_1(q)\chi_1(q,\omega)][1 - U_2(q)\chi_2(q,\omega)] - U_{12}(q)^2\chi_1(q,\omega)\chi_2(q,\omega), \tag{23}$$

where the χ's are the usual polarization functions and the U_i's are the intrasystem Coulomb interactions. The $V_{12}(q,\omega)$ can be used in placed of $U_{12}(q)$ in the above expressions for the transconductivity Eqs. (15) and (22) with no additional difficulty. Making this substitution corresponds diagrammatically to using a random-phase approximation (RPA) screened interaction between the triangles in Fig. 1(b). Most previous works[2,4,5,8,18] on drag problems have used (23) (or simplified versions of it).

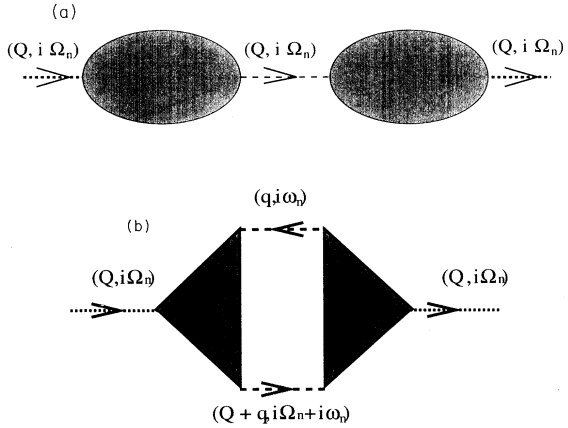

FIG. 1. Diagrams corresponding to the current-current correlation function to (a) first and (b) second order in the interlayer Coulomb interaction. The shaded triangles correspond to the Δ's given in Eqs. (17) and (18), the dashed lines to the interaction, the dotted lines to the external current operators, and the arrowheads to the direction of momentum and energy transfer.

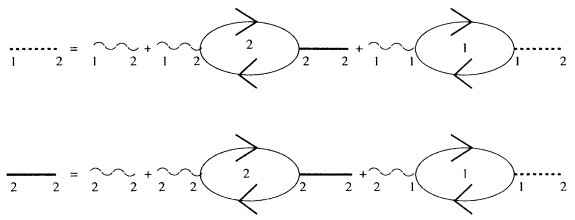

FIG. 2. Diagrams that lead to the screened interlayer interaction within the random phase approximation. The "bubbles" are the bare polarizabilities of the subsystems, the thin wavy lines are the bare interactions, the thick lines are the screened interactions, and numbers indicate the subsystem.

III. IMPURITY SCATTERING

In the preceding section we showed that the transconductivity can be expressed in terms of the general three-body correlation function Δ. We will next consider a specific example in order to calculate this three-body function, namely, noninteracting electrons scattering against random impurities. The Hamiltonian representing impurity scattering is quadratic and hence Wick's theorem is applicable, which means that the expectation value can be factorized into pairwise contractions, i.e., expressed in terms of Green functions. Impurity averaging, which is now implicit in the expectation value, reintroduces correlations between the particles, which implies that one must introduce vertex functions. However, we do not allow impurity correlations between the two subsystems, i.e., we assume that $\langle\Delta_1\Delta_2\rangle_{\rm imp} = \langle\Delta_1\rangle_{\rm imp}\langle\Delta_2\rangle_{\rm imp}$.[19] The particular choice for the impurity self-energy used in the calculation of the impurity averaged Green function fixes the choice of the vertex function; in what follows we use the self-consistent Born approximation for the self-energy and the corresponding vertex function consists either of the ladder diagrams (Sec. III C) or of the maximally crossed diagrams (Sec. III D). The form for impurity Δ giving the dominant contribution is shown in Fig. 3.[20] We consider only uniform systems and set the external wave vector to zero $\boldsymbol{Q} = 0$. We also denote fermionic complex frequencies by ik_m in contrast to bosonic frequencies $i\omega_n$ and the external frequency Ω. Thus we have

$$\Delta^\alpha(\boldsymbol{q},\boldsymbol{q};i\Omega_n\ +i\omega_n,i\omega_n) = -\frac{2}{m\nu}\sum_{\boldsymbol{k}}\frac{1}{\beta}\sum_{ik_m}k^\alpha[K(\boldsymbol{k},\boldsymbol{q},ik_m,i\Omega_n,i\omega_n) + K(\boldsymbol{k},-\boldsymbol{q},ik_m,i\Omega_n,-(i\omega_n+i\Omega_n))]\ , \tag{24}$$

where

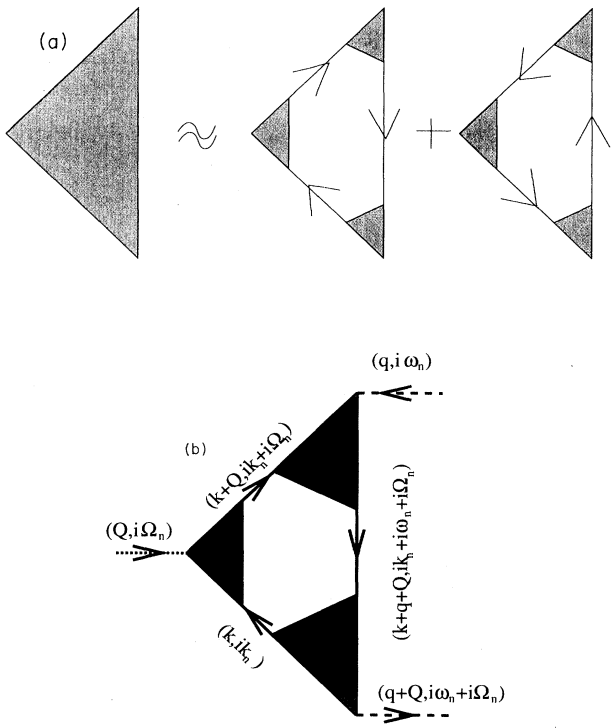

FIG. 3. Function Δ for the case in which vertex corrections are included at each of the individual charge and current vertices. (a) shows the decomposition of Δ into diagrams with clockwise- and counterclockwise-moving Green functions, with the gray shaded areas indicating vertex corrections. (b) shows one of these diagrams in greater detail. Here $k^\alpha\gamma$ is the current vertex, the Γ is the charge vertex, the dashed line is incoming momentum and frequency, the dotted lines are the interaction $V_{12}(q,\omega)$, and the solid lines with arrows are the Green function. Normal momentum and energy conservation rules apply at the vertices.

$$K(\boldsymbol{k},\boldsymbol{q},ik_m,i\Omega_n,i\omega_n) = G(\boldsymbol{k},ik_m)\gamma(\boldsymbol{k},\boldsymbol{k};ik_m,ik_m+i\Omega_n)G(\boldsymbol{k},ik_m+i\Omega_n) \times\Gamma(\boldsymbol{k},\boldsymbol{k}+\boldsymbol{q};ik_m+i\Omega_n,ik_m+i\omega_n+i\Omega_n)G(\boldsymbol{k}+\boldsymbol{q},ik_m+i\Omega_n+i\omega_n) \times\Gamma(\boldsymbol{k}+\boldsymbol{q},\boldsymbol{k};ik_m+i\omega_n+i\Omega_n,ik_m)\ . \tag{25}$$

The factor 2 in Eq. (24) comes from the spin sum. In Eq. (25), $k^\alpha\gamma/m$ is the current (vector) vertex function and Γ is the charge (scalar) vertex function. In labeling the variables in the vertex functions, we use the convention that the incoming momentum (frequency) is the first variable and the outgoing momentum (frequency) is the second variable. The second term in the square brackets in (24) corresponds to reversing the order of the two U_{12} lines; see Fig. 3. Equations (24) and (25) need to be analytically continued to the real axis, after which they can be used as a starting point for evaluating the transconductance in the weak and strong scattering limits, respectively. It should be noted that Eq. (25) does not include all possible diagrams. An example of a diagram not included is shown in Fig. 4(c).

A. Analytic continuation

The summation over the fermion frequencies ik_m follows the standard prescription:[15] the discrete sum is replaced by a contour integration $\beta^{-1}\sum_{ik_n}f(ik_n) = -(2\pi i)^{-1}\oint dz n_F(z)f(z)$. To evaluate the contour integral, one must pay attention to the branch cuts of the integrand and in the case of Eq. (24) these occur at $\mathrm{Im}[z] = 0, -\Omega_m, -\Omega_m-\omega_m$ (first term) and at $= \mathrm{Im}[z] = 0, -\Omega_m, \omega_m$ (second term). After performing the contour integration, we must further set $i\Omega_m+i\omega_m \to \Omega+\omega+i\delta$, $i\Omega_m \to \Omega+i\delta$, and $i\omega_m \to \omega - i\delta$ [see Eq. (22)]. After some tedious but straightforward algebra one finds

$$\Delta^{\alpha}(\boldsymbol{q},\Omega+\omega+i\delta,\omega-i\delta)=\frac{2}{\nu m}\sum_{\boldsymbol{k}}\int_{-\infty}^{\infty}\frac{d\epsilon}{2\pi i}n_F(\epsilon)k^{\alpha}\left\{K(\boldsymbol{k},\boldsymbol{q},\epsilon,\Omega,\omega)+K(\boldsymbol{k},-\boldsymbol{q},\epsilon,\Omega,-(\omega+\Omega))\right\}\ , \tag{26}$$

where

$$\begin{aligned}K(\mathrm{k},\boldsymbol{q},\epsilon,\Omega,\omega)=\;&G^r(\boldsymbol{k},\epsilon+\Omega)\Gamma_{++}(\boldsymbol{k},\boldsymbol{k}+\boldsymbol{q},\epsilon+\Omega,\epsilon+\omega+\Omega)G^r(\boldsymbol{k}+\boldsymbol{q},\epsilon+\omega+\Omega)\\&\times\big\{\Gamma_{++}(\boldsymbol{k}+\boldsymbol{q},\boldsymbol{k},\epsilon+\omega+\Omega,\epsilon)G^r(\boldsymbol{k},\epsilon)\gamma_{++}(\boldsymbol{k},\boldsymbol{k};\epsilon,\epsilon+\Omega)\\&-\Gamma_{+-}(\boldsymbol{k}+\boldsymbol{q},\boldsymbol{k},\epsilon+\omega+\Omega,\epsilon)G^a(\boldsymbol{k},\epsilon)\gamma_{-+}(\boldsymbol{k},\boldsymbol{k};\epsilon,\epsilon+\Omega)\big\}\\&+G^a(\boldsymbol{k}+\boldsymbol{q},\epsilon+\omega)\Gamma_{--}(\boldsymbol{k}+\boldsymbol{q},\boldsymbol{k},\epsilon+\omega,\epsilon-\Omega)G^a(\boldsymbol{k},\epsilon-\Omega)\\&\times\big\{\gamma_{-+}(\boldsymbol{k},\boldsymbol{k};\epsilon-\Omega,\epsilon)G^r(\boldsymbol{k},\epsilon)\Gamma_{+-}(\boldsymbol{k},\boldsymbol{k}+\boldsymbol{q},\epsilon,\epsilon+\omega)\\&-\gamma_{--}(\boldsymbol{k},\boldsymbol{k};\epsilon-\Omega,\epsilon)G^a(\boldsymbol{k},\epsilon)\Gamma_{--}(\boldsymbol{k},\boldsymbol{k}+\boldsymbol{q},\epsilon,\epsilon+\omega)\big\}\\&+G^a(\boldsymbol{k},\epsilon-\Omega-\omega)\gamma_{-+}(\boldsymbol{k},\boldsymbol{k};\epsilon-\Omega-\omega,\epsilon-\omega)G^r(\boldsymbol{k},\epsilon-\omega)\\&\times\big\{\Gamma_{++}(\boldsymbol{k},\boldsymbol{k}+\boldsymbol{q},\epsilon-\omega,\epsilon)G^r(\boldsymbol{k}+\boldsymbol{q},\epsilon)\Gamma_{+-}(\boldsymbol{k}+\boldsymbol{q},\boldsymbol{k},\epsilon,\epsilon-\Omega-\omega)\\&-\Gamma_{+-}(\boldsymbol{k},\boldsymbol{k}+\boldsymbol{q},\epsilon-\omega,\epsilon)G^a(\boldsymbol{k}+\boldsymbol{q},\epsilon)\Gamma_{--}(\boldsymbol{k}+\boldsymbol{q},\boldsymbol{k},\epsilon,\epsilon-\Omega-\omega)\big\}\ .\end{aligned} \tag{27}$$

Here the subscripts $\pm\pm$ indicate the signs of the (infinitesimal) imaginary parts of the vertex functions' frequency arguments. This result is still quite general and can be evaluated within different levels of approximation, of which we shall illustrate three special cases.

B. Boltzmann limit ($\omega\tau > 1$ and/or $Dq^2\tau > 1$)

In the weak scattering limit, we can neglect the charge vertex corrections, since Γ differs from unity only in a small region, where $\omega\tau$ and $Dq^2\tau$ are small. Here τ is the lifetime due to impurity scattering and D is the diffusion constant. In the dc and weak-scattering (or "Boltzmann") limit, Δ_B becomes

$$\Delta_B^{\alpha}(\boldsymbol{q},\boldsymbol{q};\omega+i\delta,\omega-i\delta)=\frac{2}{m\nu}\sum_{\boldsymbol{k}}\int_{-\infty}^{\infty}\frac{d\epsilon}{2\pi i}\,n_F(\epsilon)k^{\alpha}\big\{K_B(\boldsymbol{k},\boldsymbol{q},\epsilon,\Omega=0,\omega)+K_B(\boldsymbol{k},-\boldsymbol{q},\epsilon,\Omega=0,-\omega)\big\}\ , \tag{28}$$

where

$$\begin{aligned}K_B(\boldsymbol{k},\boldsymbol{q},\epsilon,\Omega=0,\omega)=\;&G^r(\boldsymbol{k},\epsilon)G^r(\boldsymbol{k}+\boldsymbol{q},\epsilon+\omega)[G^r(\boldsymbol{k},\epsilon)\gamma^B_{++}(\boldsymbol{k},\boldsymbol{k};\epsilon,\epsilon)-G^a(\boldsymbol{k},\epsilon)\gamma^B_{-+}(\boldsymbol{k},\boldsymbol{k};\epsilon,\epsilon)\\&+G^a(\boldsymbol{k}+\boldsymbol{q},\epsilon+\omega)G^a(\boldsymbol{k},\epsilon)[\gamma^B_{-+}(\boldsymbol{k},\boldsymbol{k};\epsilon,\epsilon)G^r(\boldsymbol{k},\epsilon)-\gamma^B_{--}(\boldsymbol{k},\boldsymbol{k};\epsilon,\epsilon)G^a(\boldsymbol{k},\epsilon)]\\&+G^a(\boldsymbol{k},\epsilon-\omega)\gamma^B_{-+}(\boldsymbol{k},\boldsymbol{k};\epsilon-\omega,\epsilon-\omega)G^r(\boldsymbol{k},\epsilon-\omega)[G^r(\boldsymbol{k}+\boldsymbol{q},\epsilon)-G^a(\boldsymbol{k}+\boldsymbol{q},\epsilon)]\\\approx\;&\gamma^B_{-+}(\boldsymbol{k},\boldsymbol{k};\epsilon_{\boldsymbol{k}},\epsilon_{\boldsymbol{k}})\big\{-G^r(\boldsymbol{k},\epsilon)G^a(\boldsymbol{k},\epsilon)[G^r(\boldsymbol{k}+\boldsymbol{q},\epsilon+\omega)-G^a(\boldsymbol{k}+\boldsymbol{q},\epsilon+\omega)]\\&+G^r(\boldsymbol{k},\epsilon-\omega)G^a(\boldsymbol{k},\epsilon-\omega)[G^r(\boldsymbol{k}+\boldsymbol{q},\epsilon)-G^a(\boldsymbol{k}+\boldsymbol{q},\epsilon)]\big\}\ .\end{aligned} \tag{29}$$

In writing the approximate equation, we used the fact that in the Boltzmann limit, (i) the terms of the form G^rG^r or G^aG^a (with equal momentum and frequency arguments) are smaller by a factor of $1/\tau E_F \ll 1$ than terms of the type G^rG^a and can hence be neglected in the present level of approximation and (ii) $G^r(\boldsymbol{k},\omega)G^a(\boldsymbol{k},\omega)=\tau A(\boldsymbol{k},\omega)$, where $A(\boldsymbol{k},\omega)$ is the spectral function and $1/2\tau=-\mathrm{Im}\Sigma^r(\boldsymbol{k},\epsilon_{\boldsymbol{k}})$. $A(\boldsymbol{k},\omega)$ is sharply peaked around $\epsilon=\epsilon_{\boldsymbol{k}}$, and hence the energy arguments in γ_{-+} can be replaced by $\epsilon_{\boldsymbol{k}}$.

In the Boltzmann limit of the current vertex function γ^B is well known:[21]

$$\gamma^B_{-+}(\boldsymbol{k},\boldsymbol{k};\epsilon_{\boldsymbol{k}},\epsilon_{\boldsymbol{k}})=\frac{\tau_{\mathrm{tr}}(\boldsymbol{k})}{\tau(\boldsymbol{k})}. \tag{30}$$

Using $G^r(\boldsymbol{k},\omega)-G^a(\boldsymbol{k},\omega)=-iA(\boldsymbol{k},\omega)$, $G^r(\boldsymbol{k},\omega)G^a(\boldsymbol{k},\omega)=\tau A(\boldsymbol{k},\omega)$, and Eq. (30), Eq. (28) thus simplifies to

$$\begin{aligned}\Delta_B^{\alpha}(\boldsymbol{q},\boldsymbol{q};\omega+i\delta,\omega-i\delta)\approx\;&\frac{2}{m\nu}\sum_{\boldsymbol{k}}\int_{-\infty}^{\infty}\frac{d\epsilon}{2\pi}\,n_F(\epsilon)k^{\alpha}\tau_{\mathrm{tr}}(\boldsymbol{k})\,[A(\boldsymbol{k},\epsilon)\,\{A(\boldsymbol{k}-\boldsymbol{q},\epsilon-\omega)+A(\boldsymbol{k}+\boldsymbol{q},\epsilon+\omega)\}\\&-A(\boldsymbol{k},\epsilon+\omega)A(\boldsymbol{k}-\boldsymbol{q},\epsilon)-A(\boldsymbol{k},\epsilon-\omega)A(\boldsymbol{k}+\boldsymbol{q},\epsilon)]\\=\;&\frac{2}{m\nu}\sum_{\boldsymbol{k}}\int_{-\infty}^{\infty}\frac{d\epsilon}{2\pi}[n_F(\epsilon+\omega)-n_F(\epsilon)]\\&\times\big[(\boldsymbol{k}+\boldsymbol{q})^{\alpha}\tau_{\mathrm{tr}}(\boldsymbol{k}+\boldsymbol{q})-\boldsymbol{k}^{\alpha}\tau_{\mathrm{tr}}(\boldsymbol{k})\big]A(\boldsymbol{k}+\boldsymbol{q},\epsilon+\omega)A(\boldsymbol{k},\epsilon)\ .\end{aligned} \tag{31}$$

The Boltzmann limit is recovered by using free Green functions, which implies that the spectral functions reduce to δ functions. We find

$$\Delta_B^\alpha(\boldsymbol{q},\boldsymbol{q};\omega+i\delta,\omega-i\delta)=\frac{2\bar{\tau}_{\rm tr}}{m}F^\alpha(\boldsymbol{q},\omega), \tag{32}$$

where the *transport polarization* F^α is given by

$$F^\alpha(\boldsymbol{q},\omega)=\frac{2}{\nu\bar{\tau}_{\rm tr}}{\rm Im}\sum_{\boldsymbol{k}}\frac{n_F(\epsilon_{\boldsymbol{k}+\boldsymbol{q}})-n_F(\epsilon_{\boldsymbol{k}})}{\epsilon_{\boldsymbol{k}+\boldsymbol{q}}-\epsilon_{\boldsymbol{k}}-\omega-i\delta} \times[(\boldsymbol{k}+\boldsymbol{q})^\alpha\tau_{\rm tr}(\boldsymbol{k}+\boldsymbol{q})-\boldsymbol{k}^\alpha\tau_{\rm tr}(\boldsymbol{k})]. \tag{33}$$

Here $\bar{\tau}_{\rm tr}$ determines the in-plane conductivity $\sigma_{ii}=e^2n_i\bar{\tau}_{{\rm tr},i}/m_i$. When (32) is inserted into the expression for the transconductivity Eq. (22) and the screening of the interlayer interaction is included as explained in Sec. II C, we obtain

$$\rho_{21}=-\frac{\sigma_{21}}{\sigma_{11}\sigma_{22}}=-\frac{1}{2n_1n_2}\frac{1}{\nu}\sum_{\boldsymbol{q}}\int_{-\infty}^{\infty}\frac{d\omega}{2\pi}\frac{\beta}{\sinh^2[\beta\omega/2]} \times|V_{12}(q,\omega)|^2F_1(\boldsymbol{q},\omega)F_2(\boldsymbol{q},\omega). \tag{34}$$

Several comments are now in order. Without an applied magnetic field, the transconductivity and consequently also the transresistivity are diagonal in the Cartesian coordinates and we have suppressed the $\{\alpha\beta\}$ indices in (34). For constant τ's transport polarization is related to the (bare) RPA polarization function $F^\alpha(\boldsymbol{q},\omega)=q^\alpha{\rm Im}\,\chi_0(\boldsymbol{q},\omega)$. In this limit Eq. (34) reproduces the standard result for transresistivity; see, e.g., Refs. 8 and 9. Since the above derivation ignores all higher-order and/or quantum-mechanical processes, it is not surprising that one can derive (34) directly from the Boltzmann equation.[13] We also emphasize that in general the drag rate, or the transresistivity, cannot be expressed in terms of the polarization function; rather, one must use the more general object F^α defined above.

C. Diffusive limit ($\omega\tau<1$, $Dq^2\tau<1$)

In this section we evaluate the transconductivity, in the weak scattering limit and in the diffusive limit ($Dq^2\tau<1$ and $\omega\tau<1$), including vertex corrections. Specifically, we consider momentum-independent relaxation times, in which case $\tau_{\rm tr}=\tau$, and include vertex corrections due to ladder diagrams. Then, we have $\gamma\equiv1$ for all $\pm$ combinations and the charge vertex is given by[22]

$$\Gamma(\boldsymbol{k},\boldsymbol{k}+\boldsymbol{q},z_1,z_2)=\frac{\theta[-{\rm Im}(z_1){\rm Im}(z_2)]}{\tau\{Dq^2-i(z_1-z_2){\rm sgn}[{\rm Im}(z_1-z_2)]\}} +\theta[{\rm Im}(z_1){\rm Im}(z_2)]\,, \tag{35}$$

where θ is the step function. It is now straightforward to use (35) in the K function (27). Including only terms that involve G^rG^a (with same arguments) and introducing a short-hand notation

$$\Gamma^\pm(q,\omega)=[\tau(Dq^2\pm i\omega)]^{-1} \tag{36}$$

allows us to write

$$K_L(\boldsymbol{k},\pm\boldsymbol{q},\epsilon,\Omega=0,\pm\omega)=G^r(\boldsymbol{k},\epsilon)G^a(\boldsymbol{k},\epsilon)\left[-G^r(\boldsymbol{k}\pm\boldsymbol{q},\epsilon\pm\omega)\Gamma^\mp(q,\omega)+G^a(\boldsymbol{k}\pm\boldsymbol{q},\epsilon\pm\omega)\Gamma^\pm(q,\omega)\right] +G^r(\boldsymbol{k},\epsilon\mp\omega)G^a(\boldsymbol{k},\epsilon\mp\omega)\left[G^r(\boldsymbol{k}\pm\boldsymbol{q},\epsilon)\Gamma^\mp(q,\omega)-G^a(\boldsymbol{k}\pm\boldsymbol{q},\epsilon)\Gamma^\pm(q,\omega)\right]. \tag{37}$$

The triangle function in the ladder approximation Δ_L^α then becomes

$$\Delta_L^\alpha(\boldsymbol{q},\boldsymbol{q},\omega+i\delta,\omega-i\delta) =\frac{2\tau}{m\nu}\sum_{\boldsymbol{k}}\boldsymbol{k}^\alpha\int_{-\infty}^{\infty}\frac{d\epsilon}{2\pi}[n_F(\epsilon+\omega)-n_F(\epsilon)] \times\{2{\rm Im}[\Gamma^-(q,\omega)G^r(\boldsymbol{k}+\boldsymbol{q},\epsilon+\omega)]A(\boldsymbol{k},\epsilon) -2{\rm Im}[\Gamma^+(q,\omega)G^r(\boldsymbol{k}-\boldsymbol{q},\epsilon)]A(\boldsymbol{k},\epsilon+\omega)\}. \tag{38}$$

We observe that the constant-τ Boltzmann result is readily recovered from (38) by replacing Γ's by unity. A generalization to energy-dependent scattering rates is straightforward, but we do not reproduce the cumbersome results here.

The next task is to establish a connection between the dressed polarization function $\chi(\boldsymbol{q},\omega)$ and the triangle function Δ_L. In Appendix C we show that

$${\rm Im}\chi(\boldsymbol{q},\omega)=-\frac{2}{\nu}\sum_{\boldsymbol{k}}{\rm Im}\left\{\int\frac{d\epsilon}{2\pi i}[n_F(\epsilon+\omega)-n_F(\epsilon)] \times\Gamma^-(q,\omega)G^r(\boldsymbol{k}+\boldsymbol{q},\epsilon+\omega)G^a(\boldsymbol{k},\epsilon)\right\}. \tag{39}$$

A comparison of (38) and (39) reveals some similarity, but clearly a few more steps are required. We complete the connection by making a few observations. First, we express the spectral functions in (38) in terms of the retarded and advanced functions. The resulting integrals can be grouped in two classes: (i) integrals involving products of the type G^rG^a and (ii) integrals involving products of the form G^rG^r or G^aG^a. We have earlier argued that type-(ii) integrals can be neglected in comparison with type-(i) integrals, if the momentum and frequency variables are equal. We now state that, in the present weak-scattering limit, this criterion applies also to functions with momentum variables and frequency variables that differ by less than $D\tau^{-1/2}$ and τ^{-1} (the diffusive limit). A proof for this statement is given in Appendix D. Thus, keeping only the G^rG^a terms in (38) allows us to express the quantity in curly brackets as

$$\{\cdots\}\to-\left[\Gamma^-(q,\omega)G^r(\boldsymbol{k}+\boldsymbol{q},\epsilon+\omega)G^a(\boldsymbol{k},\epsilon)+{\rm c.c.}\right] +\left[\Gamma^-(q,\omega)G^r(\boldsymbol{k},\epsilon+\omega)G^a(\boldsymbol{k}-\boldsymbol{q},\epsilon)+{\rm c.c.}\right].$$

In the above analysis the second term can be made to coincide with the first one by shifting the summation variable $\boldsymbol{k}\to\boldsymbol{k}+\boldsymbol{q}$; however, when doing this the pref-

actor k^α in (38) generates an extra q^α. This is exactly what is needed to give the required result,

$$\Delta_L^\alpha(q,q,\omega+i\delta,\omega-i\delta)=\frac{2\tau q^\alpha}{m}\mathrm{Im}\chi(q,\omega)\ . \tag{40}$$

The above analysis shows the equivalence of the triangle function and the polarization function in the small q and ω limit, confirming the result obtained by Zheng and MacDonald[9] with a different method. As observed by these authors, in the high-mobility samples studied so far the replacement $\chi_0 \to \chi$ does not appear to be important; however, in dirtier samples the consequences of the vertex corrections (i.e., full χ) may well become detectable.

D. Weak localization correction to Coulomb drag

In the previous sections we included the leading-order impurity scattering diagrams, which gave us the Boltzmann equation result for the case of weak scattering and showed how the bare polarization function in a certain parameter range must be replaced by the dressed polarization function. Here we develop the analysis further and calculate the quantum correction associated with weak localization (the basic physics of weak localization is reviewed, e.g., by Lee and Ramakrishnan[23]). The corrections will be of the order of $1/(k_F\ell) \ll 1$, where $\ell = v_F\tau$ is the elastic mean free path.

In Fig. 4 we display the different types of crossed diagrams that exist for the function Δ. The maximally crossed one is the one shown in Fig. 4(c). This diagram is, however, smaller than the one showed in Fig. 4(a), because of the restricted phase space. The two Green functions attached to the current vertex in the diagram in Fig. 4(a) have the same arguments because in the limit ($\boldsymbol{Q}=0,\Omega=0$) the current vertex leaves the momenta and energies of the entering and leaving Green functions unchanged. Therefore there is the possibility of two overlapping spectral functions giving a overall factor of τ. This does not happen for the diagram in Fig. 4(c). Neither does the diagram in Fig. 4(b) lead to overlapping spectral functions, except in very small regions of q,ω space, where q and ω are the incoming quantities at the charge vertices. Since we are integrating over q,ω the (logarithmic) singularity caused by the maximally crossed diagrams becomes regularized. In other words, the contribution from this diagram is small for the same reasons that the dressing of the charge vertices, discussed in Sec. III C, can be neglected for experimentally relevant parameters.[9] We therefore conclude that diagrams of the Fig. 4(a) type dominate the quantum correction to the drag rate.

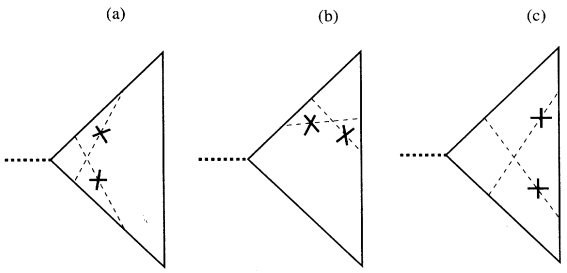

FIG. 4. Different types of crossed diagrams for the triangle diagram relevant for the weak localization correction to the transconductivity. Diagrams of the type in (a) give the leading-order contribution. Dressing the charge vertices as in (b) gives a smaller contribution for moderately clean samples for the same reason that allows us to neglect the vertex corrections of the charge vertices, discussed in Sec. III C. The diagram in (c), which cannot be included using vertex functions alone, has an even smaller phase space and can hence also be neglected.

The leading quantum correction is given as the sum of the maximally crossed diagrams, the cooperon. The resulting vertex function describing the weak localization correction, γ^{WL}, obeys

$$\gamma^{\mathrm{WL}}(\boldsymbol{k},\boldsymbol{k};ik_m,ik_m+i\Omega_n) = \frac{1}{\nu}\sum_{\boldsymbol{k}'}\frac{\boldsymbol{k}\cdot\boldsymbol{k}'}{(k')^2}G(\boldsymbol{k}',ik_m)G(\boldsymbol{k}',ik_m +i\Omega_n)C(\boldsymbol{k},\boldsymbol{k}';ik_m,ik_m+i\Omega_n), \tag{41}$$

where the cooperon is given by[24]

$$C(\boldsymbol{k},\boldsymbol{k};ik_m,ik_m+i\Omega_n) = \frac{1}{2\pi\rho\tau}\frac{1}{1-\zeta(k;ik_m,ik_m+i\Omega_n)}, \tag{42}$$

where

$$\zeta(\boldsymbol{k},\boldsymbol{k}';ik_m,ik_m+i\Omega_n) = \frac{1}{2\pi\rho\tau}\frac{1}{\nu}\sum_{\boldsymbol{p}}G(\boldsymbol{p}+\boldsymbol{Q},ik_m+i\Omega_n)G(\boldsymbol{p},ik_m), \tag{43}$$

where $\boldsymbol{Q}=\boldsymbol{k}+\boldsymbol{k}'$.

In order to evaluate the ζ function, we make use of the fact that the weak-localization divergence occurs for small Q. With this in mind we replace $\varepsilon(\boldsymbol{k}+\boldsymbol{Q})$ by $\varepsilon(\boldsymbol{k})+v_FQ\cos(\theta)$. Then we can integrate over $\boldsymbol{k}'$ in Eq. (43). For small DQ^2 and $\Omega\tau$ we obtain

$$\zeta(\boldsymbol{k},\boldsymbol{k}';ik_m,ik_m+i\Omega_n) = \begin{cases} 0 & \text{if } (k_m+\Omega_n)k_m<0 \\ 1-|\Omega_n|\tau-DQ^2\tau & \text{if } (k_m+\Omega_n)k_m>0\ , \end{cases} \tag{44}$$

where the diffusion constant is defined as $D=v_F^2\tau/2$. This expression is only valid for $Q\ell<1$, therefore the upper limit of the integral in Eq. (43) has to be cut off by $1/\ell$.

Next we perform the analytic continuations that are needed for the evaluation of the function Δ. Since the

analytic continuation $\omega_n \to \omega \pm i\delta$ leads to $|\omega_n| \to \mp i\omega$, we obtain for the ζ function

$$\begin{aligned}\zeta_{++} &= \zeta_{--} = 0,\\ \zeta_{-+}(\boldsymbol{k},\boldsymbol{k}';\epsilon,\epsilon+\Omega) &= \zeta_{-+}(\boldsymbol{k},\boldsymbol{k}';\epsilon-\Omega,\epsilon)\\ &= 1 + i\Omega\tau - DQ^2\tau.\end{aligned} \tag{45}$$

The cooperon that enters the expression for $K_{\rm WL}$, Eq. (27), then acquires the familiar form

$$C_{-+} = \frac{1}{2\pi\rho\tau^2}\frac{1}{-i\Omega + DQ^2}. \tag{46}$$

After integration over $\boldsymbol{Q}$ we find the weak-localization vertex function

$$\begin{aligned}\gamma^{\rm WL}(\boldsymbol{k},\boldsymbol{k};\epsilon-\Omega,\epsilon) &= \gamma^{\rm WL}(\boldsymbol{k},\boldsymbol{k};\epsilon,\epsilon+\Omega)\\ &\approx A(k,\epsilon)\frac{1}{\pi k_F \ell\tau}\ln(\Omega\tau)\\ &\equiv A(k,\epsilon)\eta^{\rm WL}(\Omega)/2\tau.\end{aligned} \tag{47}$$

Here $\eta^{\rm WL}$ is the ratio between the quantum correction and the classical conductivity: $\eta^{\rm WL}(\Omega) = \delta\sigma(\omega)/\sigma_0$.[24] The combinations $\gamma^{\rm WL}_{++}$ and $\gamma^{\rm WL}_{--}$ are both zero. We now get for the K function

$$\begin{aligned}K_{\rm WL}(\boldsymbol{k},\boldsymbol{q};\epsilon,\Omega,\omega) \approx -i\eta^{\rm WL}\{&-[A(\boldsymbol{k},\epsilon)]^2 A(\boldsymbol{k}+\boldsymbol{q},\epsilon+\omega)\\ &+[A(\boldsymbol{k},\epsilon-\omega)]^2 A(\boldsymbol{k}+\boldsymbol{q},\epsilon)\}\ .\end{aligned} \tag{48}$$

Using that $A^2 \approx \tau A/2$ for large τ we can express the weak-localization correction $\delta\Delta_{\rm WL}$ in terms of the response functions as

$$\begin{aligned}&\delta\Delta^{\alpha}_{\rm WL}(\boldsymbol{q},\boldsymbol{q};\omega+i\delta,\omega-i\delta,\Omega)\\ &\quad= \frac{2\tau\eta^{\rm WL}(\Omega)}{m}\, q^{\alpha}\,{\rm Im}\,\chi_0(\boldsymbol{q},\omega)\\ &\quad= \eta^{\rm WL}(\Omega)\Delta^{\alpha}_{\rm B}(\boldsymbol{q},\boldsymbol{q};\omega+i\delta,\omega-i\delta),\end{aligned} \tag{49}$$

which immediately leads to the conclusion that to leading order the weak-localization correction to transconductance is

$$\delta\sigma^{\rm WL}_{21}(\Omega) = [\eta^{\rm WL}_1(\Omega) + \eta^{\rm WL}_2(\Omega)]\sigma^0_{21}. \tag{50}$$

Consequently, the transresistance is *unaffected* by the weak-localization correction because

$$\rho_{21} \approx -\frac{\sigma^0_{21}(1+\eta_1+\eta_2)}{\sigma^0_{11}(1+\eta_1)\sigma^0_{22}(1+\eta_2)} \approx \rho^0_{21}. \tag{51}$$

Weak localization is strongly affected by external magnetic fields. The formalism presented above can be extended to include magnetic fields; in particular, the topology of all diagrams remains unaltered.

IV. FINITE-FREQUENCY RESPONSE AT $T = 0$

A. General expression

For finite frequencies and finite temperatures the analysis becomes considerably more complicated and for simplicity we therefore restrict ourselves to study the finite-frequency case at zero temperature. Furthermore, we will consider a model where all vertex functions can be replaced by unity, i.e., a system with short-range impurity potentials and a system not in the diffusive limit. The transconductivity in terms of the time-ordered current-current correlation function is

$$\begin{aligned}\sigma^{\alpha\beta}(\boldsymbol{Q},\Omega) = \frac{e^2}{\Omega}\{&i{\rm Re}\,[\Pi^{\alpha\beta,t}(\boldsymbol{Q},\Omega)]\\ &-{\rm sgn}(\Omega){\rm Im}\,[\Pi^{\alpha\beta,t}(\boldsymbol{Q},\Omega)]\}.\end{aligned} \tag{52}$$

The time-ordered current-current correlation function is now written in terms of time-ordered Green functions as

$$\begin{aligned}\Pi^{\alpha\beta,t}(\boldsymbol{Q}=0,\Omega) = -\frac{i}{2}\int\frac{d\omega}{2\pi}\frac{1}{\nu}\sum_{\boldsymbol{q}} &V_{12}(q,\omega)V^*_{12}(q,\omega+\Omega)\\ &\times\Delta^{\alpha,t}(\boldsymbol{q},\boldsymbol{q};\Omega+\omega,\omega)\\ &\times\Delta^{\beta,t}(-\boldsymbol{q},-\boldsymbol{q};-\Omega-\omega,-\omega),\end{aligned} \tag{53}$$

where

$$\begin{aligned}&\Delta^{\alpha,t}(\boldsymbol{q},\boldsymbol{q};\Omega+\omega,\omega)\\ &\quad= \int\frac{d\omega_1}{2\pi}\frac{2}{\nu}\sum_{\boldsymbol{k}} v_{\alpha}(\boldsymbol{k})G^t(\boldsymbol{k},\omega_1+\tfrac{1}{2}\Omega)G^t(\boldsymbol{k},\omega_1-\tfrac{1}{2}\Omega)\\ &\qquad\times\left[G^t(\boldsymbol{k}+\boldsymbol{q},\omega_1+\omega)+G^t(\boldsymbol{k}-\boldsymbol{q},\omega_1-\omega)\right].\end{aligned} \tag{54}$$

It is straightforward to see that $\Delta^{\alpha,t}(\boldsymbol{q},\boldsymbol{q};\omega,\omega) = 0$, which can be shown along the same lines as in the last part of Appendix B. Furthermore, we can show that $\Delta(\boldsymbol{q},\boldsymbol{q};\omega,\omega+\Omega)$ is proportional to Ω and consequently the transconductivity vanishes at zero frequency and zero temperature in agreement with Eq. (22).

B. Clean system

To evaluate the zero-temperature correlation function it is useful to decompose the time-ordered Green function into advanced and retarded parts according to $G^t(\boldsymbol{q},\omega) = \Theta(\omega)G^r(\boldsymbol{q},\omega) + \Theta(-\omega)G^a(\boldsymbol{q},\omega)$. In the case of a clean system, the decomposition can also be carried out in momentum space as $G^t(\boldsymbol{q},\omega) = \Theta(|\boldsymbol{q}|-k_F)G^r(\boldsymbol{q},\omega) + \Theta(k_F-|\boldsymbol{q}|)G^a(\boldsymbol{q},\omega)$, which is actually more convenient since it leaves the frequency integrals unrestricted. Consequently, using the momentum space decomposition, we can carry out the conventional pole-position analysis and find that most of the terms arising from (53) vanish. The remaining nonzero terms are most conveniently evaluated using the frequency-space decomposition, which yields for $\Omega > 0$

$$\Pi^{\alpha\alpha,t}(\boldsymbol{Q}=0,\Omega) = -\frac{4i}{\nu^3}\sum_{\boldsymbol{q},\boldsymbol{p},\boldsymbol{k}} V_{12}(q,\omega)V_{12}^*(q,\omega+\Omega)v_\alpha(\boldsymbol{k})v_\alpha(\boldsymbol{p})$$
$$\times\Bigg\{2\int_{-\Omega/2}^{\Omega/2}\frac{d\omega_1}{2\pi}\int_{-\Omega/2}^{\omega_1}\frac{d\omega_2}{2\pi}\int_{\omega_2}^{\omega_1}\frac{d\omega}{2\pi}G^r(\boldsymbol{k},\omega_1+\tfrac{1}{2}\Omega)G^a(\boldsymbol{k},\omega_1-\tfrac{1}{2}\Omega)$$
$$\times G^r(\boldsymbol{k}-\boldsymbol{q},\omega_1-\omega)G^r(\boldsymbol{p},\omega_2+\tfrac{1}{2}\Omega)G^a(\boldsymbol{p},\omega_2-\tfrac{1}{2}\Omega)G^a(\boldsymbol{p}-\boldsymbol{q},\omega_2-\omega)$$
$$+\int_{-\Omega/2}^{\Omega/2}\frac{d\omega_1}{2\pi}\int_{-\omega_1}^{\Omega/2}\frac{d\omega_2}{2\pi}\int_{-\omega_2}^{\omega_1}\frac{d\omega}{2\pi}G^r(\boldsymbol{k},\omega_1+\tfrac{1}{2}\Omega)G^a(\boldsymbol{k},\omega_1-\tfrac{1}{2}\Omega)$$
$$\times G^r(\boldsymbol{k}-\boldsymbol{q},\omega_1-\omega)G^r(\boldsymbol{p},\omega_2+\tfrac{1}{2}\Omega)G^a(\boldsymbol{p},\omega_2-\tfrac{1}{2}\Omega)G^r(\boldsymbol{p}+\boldsymbol{q},\omega_2+\omega)$$
$$+\int_{-\Omega/2}^{\Omega/2}\frac{d\omega_1}{2\pi}\int_{-\omega_1}^{-\omega_2}\frac{d\omega_2}{2\pi}\int_{\omega_1}^{-\omega_2}\frac{d\omega}{2\pi}G^r(\boldsymbol{k},\omega_1+\tfrac{1}{2}\Omega)G^a(\boldsymbol{k},\omega_1-\tfrac{1}{2}\Omega)$$
$$\times G^a(\boldsymbol{k}-\boldsymbol{q},\omega_1-\omega)G^r(\boldsymbol{p},\omega_2+\tfrac{1}{2}\Omega)G^a(\boldsymbol{p},\omega_2-\tfrac{1}{2}\Omega)G^a(\boldsymbol{p}+\boldsymbol{q},\omega_2+\omega)\Bigg\}. \quad (55)$$

Since all frequency integrations run at most over an interval of length Ω, the end result is proportional to Ω^3. We can furthermore show that $\Pi^{\alpha\alpha,t}(\boldsymbol{Q},\Omega)=\Pi^{\alpha\alpha,t}(\boldsymbol{Q},-\Omega)$, so that $\Pi^{\alpha\alpha,t}(\boldsymbol{Q},\Omega)\sim|\Omega|^3$. Using the fluctuation-dissipation theorem we find Re $\Pi^r\sim|\Omega|^3$ and Im $\Pi^r\sim\Omega^3$. Thus, to a leading order in τ, the real part of the transconductivity is proportional to Ω^2 and its imaginary part is proportional to $\mathrm{sgn}(\Omega)\Omega^2$.

C. Disordered systems

For disordered systems we can only use the frequency-space decomposition and consequently the pole-position analysis is not quite as powerful as for clean systems. We can, however, determine the leading corrections by regarding τ^{-1} as a perturbation and using a Taylor expansion of the type $G^r(\omega_1)G^r(\omega_1)G^r(\omega_1-\omega)=G_0^r(\omega_1)G_0^r(\omega_1)G_0^r(\omega_1-\omega)+(i/2\tau)(\partial/\partial\omega_1)[G_0^r(\omega_1)G_0^r(\omega_1)G_0^r(\omega_1-\omega)]$. After the expansion, all propagators are given by clean system Green functions and we can easily do the integral over one of the frequency arguments (in the example over ω_1). The resulting term is identical with a term that is encountered in the evaluation of an auxiliary time-ordered function for a clean system. The auxiliary function can be analyzed also by means of the momentum-space decomposition (since all propagators are given by G_0^t) and the frequency dependence of the various terms can be obtained in a manner similar to what we did in the clean system case. Carrying out the analysis for all terms arising from (53), we find that the leading-order corrections to Π^t are of the form Ω^2/τ and we obtain

$$\Pi^t(\boldsymbol{Q},\Omega)=F_0(\boldsymbol{Q})|\Omega|^3+F_1(\boldsymbol{Q})\Omega^2/\tau. \quad (56)$$

Thus we finally have

$$\sigma_{21}(\boldsymbol{Q}=0,\Omega)\sim\begin{cases}\Omega, & |\Omega|\ll 1/\tau\\ \Omega^2, & 1/\tau\ll|\Omega|\ll\epsilon_F/\hbar\end{cases}. \quad (57)$$

The constant $F_0(0)$ can be evaluated approximately be keeping only the most important terms. Taking only terms that are leading order in τ into account, we find

$$F_0(0)=-i\frac{2\tau^2}{3(2\pi)^3}\left(\frac{k_F}{v_F}\right)^2\int_0^{2\pi}\frac{d\theta}{2\pi}[1-\cos(\theta)]$$
$$\times|V_{12}(k_F\sqrt{2-2\cos(\theta)},\omega=0)|^2\,. \quad (58)$$

Here the remaining integral is strongly reminescent of the ratio between a scattering time and a transport time, the only difference being that instead of an impurity potential the integrand now contains the potential due to carriers in the other subsystem.

V. DISCUSSION AND CONCLUSIONS

In this paper, we have presented a fully microscopic theory of the Coulomb drag, based on the Kubo formalism. We have used the finite-temperature formalism to obtain expressions for the dc drag and the zero-temperature formalism to obtain finite-frequency results. We have chosen to present only formal results here, deferring the presentation of experimental consequences of these results to another work.[13]

We calculate the transconductivity σ_{12} using an order by order expansion in the interlayer interaction $U(\boldsymbol{q})$. Assuming no correlations between the impurities between the two layers, we find an exact relation between the first-order result $\sigma_{12}^{(1)}(\boldsymbol{q},\omega)$ and the subsystem conductivities. The result also indicates that in a uniform system, the dc transconductivity vanishes to first order.

To second order, we write a formal result for the transconductivity $\sigma_{12}^{(2)}$ in terms of the $\Delta(\boldsymbol{q},\boldsymbol{q}';\omega,\omega')$ functions, which are the thermal-averaged $\langle j\rho\rho\rangle$ correlation functions of the individual subsystems. In evaluating Δ under various circumstances, we find (i) for *constant* intralayer elastic scattering rates, we duplicate in the limit $1/\tau\to 0$ results obtained earlier using the Boltzmann equation and the memory functional method in the diffusive limit; (ii) for *energy-dependent* intralayer elastic scattering rates, however, the $q^\alpha\mathrm{Im}[\chi]$ must be replaced by another quantity $F^\alpha(\boldsymbol{q},\omega)$, which we call the transport polarizability. The energy-dependent result is due

(from the Boltzmann equation point of view) to the fact that the perturbed distribution function on application of the electric field for energy-dependent elastic scattering rates is not a drifted Fermi-Dirac function.[13] However, intralayer electron-electron interactions tend to relax the distribution function back to a drifted Fermi-Dirac function and hence the larger the intralayer electron-electron interactions are, the closer the $F^{\alpha}(\boldsymbol{q},\omega)$ will be to $q^{\alpha}\mathrm{Im}[\chi_0]$ in Eq. (34).[13]

We have calculated the weak-localization correction to the second-order transconductivity and found that $\delta\sigma_{21}^{\mathrm{WL}}/\sigma_{21}^{0} = \delta\sigma_{11}^{\mathrm{WL}}/\sigma_{11}^{0} + \delta\sigma_{22}^{\mathrm{WL}}/\sigma_{22}^{0}$, which implies that, to lowest order in $(k_F\ell)^{-1}$, the *transresistivity* ρ_{21} is *unaffected* by the weak-localization corrections. The zero-temperature formalism indicates that the dc drag vanishes in an open system. This result is reproduced in the $T \to 0$ of the finite temperature formalism, since the $\partial_{\omega} n_B(\omega)$ term in Eq. (22) vanishes as $T \to 0$ and one can show that Δ is linear in ω as $\omega \to 0$. This statement is valid for open systems, which are connected to dissipative leads, and not for closed systems.[14]

For finite frequencies we have evaluated the leading contribution to the transconductivity at zero temperature and found that in the clean limit $\sigma_{21} \sim \Omega^2$. Including disorder we showed that frequency in this expression is replaced by $1/\tau$ and $\sigma_{21} \sim \Omega/\tau$.

The formalism that we have developed in this paper can be applied to many different physical realizations of coupled electron systems. It is thus straightforward to extend the calculation to include magnetic field and work is in progress in this direction.[25] The present formalism also forms a useful starting point for the study of, e.g., higher-order intralayer interactions, phonon mediated intralayer interaction, and correlations caused by strong interlayer electron-electron interactions.

ACKNOWLEDGMENTS

We thank Martin Bønsager, D. E. Khmelnitskii, P. A. Lee, and Lu Sham for useful comments and discussions. K.F. was supported by the Carlsberg Foundation. We recently became aware of work done by Alex Kamenev and Yuval Oreg on the same subject.[27]

APPENDIX A: BRANCH CUTS FOR THE THREE-BODY CORRELATION FUNCTION

Consider the Fourier transform in time according to Eq. (18) (we set $\tau'' = 0$ since Δ is only a function of $\tau - \tau''$ and $\tau' - \tau''$)

$$\Delta(i\Omega_n + i\omega_n, i\omega_n) = \int_0^{\beta} d\tau \int_0^{\beta} d\tau'\, e^{i\Omega_n\tau + i\omega_n\tau'} \Delta(xx'x''; \tau\tau')$$
$$= \int_0^{\beta} d\tau\, e^{i\Omega_n\tau} \left(\int_0^{\tau} d\tau'\, e^{i\omega_n\tau'} \langle J(x\tau)\rho(x'\tau')\rho(x'')\rangle + \int_{\tau}^{\beta} d\tau'\, e^{i\omega_n\tau'} \langle \rho(x'\tau')J(x\tau)\rho(x'')\rangle \right). \quad \text{(A1)}$$

We now insert the identity $1 = \sum_n |n\rangle\langle n|$, where $\{|n\rangle\}$ is a set of eigenstates for the Hamiltonian, between the operators in Eq. (A1). After performing the two imaginary time integrals and some algebra we obtain

$$\Delta(i\Omega_n + i\omega_n, i\omega_n) = e^{\beta\Omega} \sum_{k,m,l} \Bigg[\langle k|J(x)|m\rangle\langle m|\rho(x')|l\rangle\langle l|\rho(x'')|k\rangle \frac{1}{i\omega_n + E_m - E_l}$$
$$\times \left\{ \frac{1}{i\Omega_n + i\omega_n + E_k - E_l} \left(e^{-\beta E_l} - e^{-\beta E_k}\right) + \frac{1}{i\Omega_n + E_k - E_m} \left(e^{-\beta E_k} - e^{-\beta E_m}\right) \right\}$$
$$+ \langle m|J(x)|k\rangle\langle l|\rho(x')|m\rangle\langle k|\rho(x'')|l\rangle \frac{1}{i\omega_n + E_l - E_m}$$
$$\times \left\{ \frac{1}{i\Omega_n + i\omega_n + E_l - E_k} \left(e^{-\beta E_l} - e^{-\beta E_k}\right) + \frac{1}{i\Omega_n + E_m - E_k} \left(e^{-\beta E_k} - e^{-\beta E_m}\right) \right\} \Bigg] . \quad \text{(A2)}$$

From this expression we can read of the branch cuts of $\Delta(i\Omega_n + i\omega_n, i\omega_n)$, which is used when doing the Matsubara sum over $i\omega_n$ in Eq. (20a).

APPENDIX B: PROOF OF $\Delta(++) = 0$

We consider the quantity

$$\bar{\Delta}(\boldsymbol{x}', i\Omega_n + i\omega_n, i\omega_n)$$
$$= \int_0^{\beta} d\tau' \int_0^{\beta} d\tau\, e^{i\Omega_n\tau} e^{i\omega_n\tau'} \langle T[J(\tau)\rho(\boldsymbol{x}'\tau')\rho(0)]\rangle, \quad \text{(B1)}$$

where $J = \int d\boldsymbol{x} j_{\mu}(\boldsymbol{x})$. The Fourier of $\bar{\Delta}(\boldsymbol{x}', i\Omega_n + i\omega_n, i\omega_n)$ with respect to $\boldsymbol{x}'$ is $\Delta(\boldsymbol{q},\boldsymbol{q}; i\Omega_n + i\omega_n, i\omega_n)$.

We need the two combinations $\Delta(+-)$ and $\Delta(++)$. It is clear that if we set $i\Omega_n = 0$ in expression above we lose the information necessary to evaluate $\Delta(+-)$ and we can only get $\Delta(++)$ by the substitution $i\omega_n \to \omega + i\delta$. The dc limit of $\Delta(++)$ can be safely evaluated by setting $i\Omega_n = 0$ before the analytic continuation. Doing that we obtain

$$\bar{\Delta}(\boldsymbol{x}', i\omega_n, i\omega_n) = \beta \int_0^{\beta} d\tau'\, e^{i\omega_n\tau'} \langle T[J(\tau)\rho(\boldsymbol{x}'\tau')\rho(0)]\rangle. \quad \text{(B2)}$$

Now consider the density-density correlation function for the case when the Hamiltonian has been enlarged by a vector potential term

$$H \to H + A_\mu J_\mu \tag{B3}$$

(omitting a diamagnetic term that is not important for the present argument). If we view A_μ as a perturbation we can write the charge-charge correlation function as

$$\chi_A(\boldsymbol{x}',\tau') = \left\langle T\left[\exp\left(-\int_0^\beta d\tau A_\mu J_\mu(\tau)\right) \times\rho(\boldsymbol{x}'\tau')\rho(0)\right]\right\rangle. \tag{B4}$$

From this expression it is seen that the function $\bar{\Delta}$ can be obtained as

$$\bar{\Delta}_\mu(\boldsymbol{x}',\tau') = -\left.\frac{d\chi_A(\boldsymbol{x}',\tau')}{dA_\mu}\right|_{A_\mu=0}. \tag{B5}$$

Since a constant vector potential can always be removed by a gauge transformation (this is, however, only strictly true for a system with open boundary conditions), χ_A cannot depend on A and hence we arrive at the conclusion that $\bar{\Delta} = 0$.

As a specific example we now take the impurity averaged $\Delta(++)$ function in the simplifying case where we can neglect the charge vertex corrections (i.e., not in the diffusive limit). Setting $i\Omega_n = 0$ in Eq. (25), we then have

$$\begin{aligned}
&\frac{k^\alpha}{m}K(\boldsymbol{k},\boldsymbol{q},ik_m,i\omega_n)\\
&\quad= [G(\boldsymbol{k},ik_m)]^2\frac{k^\alpha}{m}\gamma(\boldsymbol{k};ik_m)G(\boldsymbol{k}+\boldsymbol{q},ik_m+i\omega_n)\\
&\quad= -\frac{\partial G(\boldsymbol{k},ik_m)}{\partial k^\alpha}G(\boldsymbol{k}+\boldsymbol{q},ik_m+i\omega_n),
\end{aligned}$$

where we have used the Ward identity $\partial_{\boldsymbol{k}}G^{-1}(\boldsymbol{k},ik_m) = \boldsymbol{k}\gamma(\boldsymbol{k},ik_m)/m$. Integrating by parts, we obtain

$$\begin{aligned}
&\Delta^\alpha(\boldsymbol{q},\boldsymbol{q},;i\omega_n,i\omega_n)\\
&= \frac{\partial}{\partial q^\alpha}\frac{e}{m}\frac{1}{\beta}\sum_{ik_m}\int\frac{d\boldsymbol{k}}{(2\pi)^2}\left[G(\boldsymbol{k},ik_m)G(\boldsymbol{k}+\boldsymbol{q},ik_m\right.\\
&\quad\left.+i\omega_n) - G(\boldsymbol{k},ik_m)G(\boldsymbol{k}-\boldsymbol{q},ik_m-i\omega_n)\right] = 0,
\end{aligned} \tag{B6}$$

which can be seen by shifting ik_n and $\boldsymbol{k}$ in the second term.

APPENDIX C: IMAGINARY PART OF THE POLARIZABILITY IN THE DIFFUSIVE LIMIT

In this appendix, we derive expressions for $\mathrm{Im}[\chi]$ when $qv_F\tau < 1$ and $\omega\tau < 1$, i.e, in the diffusive limit. The polarizability including the vertex correction Γ is given by

$$\begin{aligned}
\chi(q,i\omega_n) = \frac{2}{\nu\beta}\sum_{\boldsymbol{k}}\sum_{i\varepsilon_n} &G(\boldsymbol{k}+\boldsymbol{q},i\varepsilon_n+i\omega_n)\\
&\times G(\boldsymbol{k},i\varepsilon_n)\Gamma(q;i\varepsilon_n+i\omega_n,i\varepsilon_n).
\end{aligned} \tag{C1}$$

For $qv_F\tau < 1$ and $\omega\tau < 1$, Γ is given by Eq. (35). Inserting this form of the vertex correction in Eq. (C1), writing the sum as a contour integral, and deforming the contour in the standard manner[15] yields

$$\begin{aligned}
\chi(q,\omega) = -\frac{2}{\nu}\sum_{\boldsymbol{k}}\int\frac{d\varepsilon}{2\pi i}\, n_F(\varepsilon)\{&[\Gamma^-(q,\omega)G^r(\boldsymbol{k}+\boldsymbol{q},\varepsilon)\\
&-G^a(\boldsymbol{k}+\boldsymbol{q},\varepsilon)]G^a(\boldsymbol{k},\varepsilon-\omega)\\
&+[G^r(\boldsymbol{k},\varepsilon)-\Gamma^-(q,\omega)G^a(\boldsymbol{k},\varepsilon)]\\
&\times G^r(\boldsymbol{k}+\boldsymbol{q},\varepsilon+\omega)\}.
\end{aligned} \tag{C2}$$

In the above equation, the analytic continuation $i\omega_n \to \omega + i0^+$ has been taken and $\Gamma^\pm(q,\omega)$ is defined in Eq. (36).

We write $\chi = \chi_a + \chi_b$, where χ_a (χ_b) excludes (includes) the vertex corrections. The term χ_a to lowest order in q and ω is

$$\begin{aligned}
\chi_a(q,\omega) &\equiv -\frac{2}{\nu}\sum_{\boldsymbol{k}}\int\frac{d\varepsilon}{2\pi i}n_F(\varepsilon)\left[G^r(\boldsymbol{k},\varepsilon)G^r(\boldsymbol{k}+\boldsymbol{q},\varepsilon+\omega)\right.\\
&\quad\left.-G^a(\boldsymbol{k}+\boldsymbol{q},\varepsilon)G^a(\boldsymbol{k},\varepsilon-\omega)\right]\\
&\approx \frac{2}{\nu}\sum_{\boldsymbol{k}}\int\frac{d\varepsilon}{2\pi i}n_F(\varepsilon)\frac{\partial[G^r(\boldsymbol{k},\varepsilon)-G^a(\boldsymbol{k},\varepsilon)]}{\partial\varepsilon}\\
&= -\int\frac{d\varepsilon}{2\pi i}n_F'(\varepsilon)\frac{2}{\nu}\sum_{\boldsymbol{k}}[G^r(\boldsymbol{k},\varepsilon)-G^a(\boldsymbol{k},\varepsilon)]\\
&= -\frac{\partial n}{\partial\mu}.
\end{aligned} \tag{C3}$$

Note that χ_a to lowest order in q and ω is purely real.

The second part is

$$\begin{aligned}
\chi_b(q,\omega) = -\Gamma^-(q,\omega)\frac{2}{\nu}\sum_{\boldsymbol{k}}\int\frac{d\varepsilon}{2\pi i}&n_F(\varepsilon)\\
&\times[G^r(\boldsymbol{k}+\boldsymbol{q},\varepsilon)G^a(\boldsymbol{k},\varepsilon-\omega)\\
&-G^a(\boldsymbol{k},\varepsilon)G^r(\boldsymbol{k}+\boldsymbol{q},\varepsilon+\omega)].
\end{aligned} \tag{C4}$$

To lowest order in q and ω, this is[26]

$$\chi_b(q,\omega) = \frac{\partial n}{\partial\mu}\frac{-i\omega}{Dq^2-i\omega}. \tag{C5}$$

Thus χ_b has an imaginary component, which, as shown in Sec. III, is related to the Δ when $qv_F\tau < 1$ and $\omega\tau < 1$.

APPENDIX D: JUSTIFICATION FOR NEGLECTING G^RG^R AND G^AG^A TERMS

In this appendix, we show that the terms in Δ_L involving products G^rG^r and G^aG^a (denoted below as Δ_s) can be neglected when compared to G^aG^r when $E_F\tau \gg 1$, in the diffusive limit. Written in full, Δ_s is

$$\Delta_s^\alpha(q,q;\omega'+i\delta,\omega'-i\delta) = -\frac{2\tau}{m}\frac{1}{\nu}\sum_{\boldsymbol{k}}\int\frac{d\varepsilon}{2\pi}n_F(\varepsilon)k^\alpha\{\Gamma^-(q,\omega)[-G^r(\boldsymbol{k},\varepsilon)G^r(\boldsymbol{k}+\boldsymbol{q},\varepsilon+\omega)-G^a(\boldsymbol{k},\varepsilon)G^a(\boldsymbol{k}-\boldsymbol{q},\varepsilon-\omega) +G^r(\boldsymbol{k},\varepsilon-\omega)G^r(\boldsymbol{k}+\boldsymbol{q},\varepsilon)+G^a(\boldsymbol{k},\varepsilon+\omega)G^a(\boldsymbol{k}-\boldsymbol{q},\varepsilon)]+\text{c.c.}\}\ . \tag{D1}$$

Note that at $\omega=0$, this term is identically zero. Expanding in powers of ω gives

$$\begin{aligned}\Delta_s^\alpha(q,q;\omega'+i\delta,\omega'-i\delta) &= \mathrm{Re}\Bigg[-\omega\Gamma^-(q,\omega)\frac{\tau}{m}\frac{4}{\nu}\sum_{\boldsymbol{k}}\int\frac{d\varepsilon}{2\pi}n_F(\varepsilon)\,k^\alpha \\ &\quad\times\frac{\partial[G^a(\boldsymbol{k},\varepsilon)G^a(\boldsymbol{k}-\boldsymbol{q},\varepsilon)-G^r(\boldsymbol{k},\varepsilon)G^r(\boldsymbol{k}+\boldsymbol{q},\varepsilon)]}{\partial\varepsilon}+O(\omega^2)\Bigg] \\ &= \mathrm{Re}\Bigg[-\omega\Gamma^-\frac{\tau}{m}\frac{4}{\nu}\sum_{\boldsymbol{k}}\int\frac{d\varepsilon}{2\pi}n_F'(\varepsilon)k^\alpha[G^a(\boldsymbol{k},\varepsilon)G^a(\boldsymbol{k}-\boldsymbol{q},\varepsilon)-G^r(\boldsymbol{k},\varepsilon)G^r(\boldsymbol{k}+\boldsymbol{q},\varepsilon)]\Bigg]+O(\omega^2).\end{aligned} \tag{D2}$$

Expanding Eq. (D2) in powers of q and assuming that the self-energy is small (since τ is large) so that $\partial G/\partial\varepsilon_{\boldsymbol{k}}\approx G^2$, yields

$$\Delta_s^\alpha(q,q;\omega'+i\delta,\omega'-i\delta) = \mathrm{Re}\Bigg[\omega q^\alpha\Gamma^-(q,\omega)\frac{\tau}{m}\frac{4}{\nu}\sum_{\boldsymbol{k}}\int\frac{d\varepsilon}{2\pi}n_F'(\varepsilon)\frac{(k^\alpha)^2}{m}[G^a(\boldsymbol{k},\varepsilon)^3+G^r(\boldsymbol{k},\varepsilon)^3]\Bigg]+O(q^2,\omega^2). \tag{D3}$$

Integrals of $G^{a,r}(\boldsymbol{k},\varepsilon)^3$ over $\boldsymbol{k}$ do *not* diverge when $\tau\to\infty$ because the poles of the function are on the same half-plane [unlike integrals over $G^a(\boldsymbol{k},\varepsilon)G^r(\boldsymbol{k},\varepsilon)$, which go as τ]. Since $n_F'(\varepsilon)$ is peaked around μ, one can estimate the magnitude of Δ_s^α by replacing $-n_F'(\varepsilon)\approx\delta(\varepsilon-\mu)$, which gives

$$\Delta_s^\alpha(q,q';\omega'+i\delta,\omega'-i\delta)\approx\mathrm{Re}\Bigg[\Gamma^-(q,\omega)\frac{e\tau q^\alpha\omega}{2\pi^3E_F}\Bigg]. \tag{D4}$$

A comparison of this with Δ_L^α given in Eq. (40) shows that Δ_s^α is smaller by a factor of $1/(E_F\tau)$.

---

* Present address: Dansk Institut for Fundamental Metrologi, Anker Engelundsvej 1, DK-2800 Lyngby, Denmark.

† Present address: Institut för Tillämpad Fysik, Chalmers Tekniska Högskola och Göteborgs Universitet, S-41296 Göteborg, Sweden.

[1] T. J. Gramila, J. P. Eisenstein, A. H MacDonald, L. N. Pfeiffer, and K. W. West, Phys. Rev. Lett. **66**, 1216 (1991); Phys. Rev. B **47**, 12 957 (1993); Physica B **197**, 442 (1994).

[2] U. Sivan, P. M. Solomon, and H. Shtrikman, Phys. Rev. Lett. **68**, 1196 (1992).

[3] P. M. Solomon, P. J. Price, D. J. Frank, and D. C. L. Tulipe, Phys. Rev. Lett. **63**, 2508 (1989).

[4] H. C. Tso, P. Vasilopoulos, and F. M. Peeters, Phys. Rev. Lett. **68**, 2516 (1992); **70**, 2146 (1993); H. C. Tso and P. Vasilopoulos, Phys. Rev. B **45**, 1333 (1992).

[5] K. Flensberg and B. Y.-K. Hu, Phys. Rev. Lett. **73**, 3572 (1994).

[6] M. B. Pogrebinskii, Fiz. Tekh. Poluprovodn. **11**, 637 (1977) [Sov. Phys. Semicond. **11**, 372 (1977)].

[7] P. J. Price, Physica B **117**, 750 (1983).

[8] A.-P. Jauho and H. Smith, Phys. Rev. B **47**, 4420 (1993).

[9] L. Zheng and A. H. MacDonald, Phys. Rev. B **48**, 8203 (1993).

[10] L. G. Aslamazov and A. I. Larkin, Fiz. Tverd. Tela (Leningrad) **10**, 1104 (1968) [Sov. Phys. Solid State **10**, 875 (1968)].

[11] K. Rapcewicz and N. W. Ashcroft, Phys. Rev. B **44**, 4032 (1991).

[12] R. E. Goldstein, G. Parola, and A. P. Smith, J. Chem. Phys. **91**, 1843 (1989).

[13] K. Flensberg and B. Y.-K. Hu, Phys. Rev. B **52**, 14 796 (1995).

[14] A. G. Rojo and G. D. Mahan, Phys. Rev. Lett. **68**, 2074 (1992).

[15] G. D. Mahan, *Many-Particle Physics* (Plenum, New York, 1990).

[16] For a system where the two subsystems scatter from the same impurities, diagrams that connect the two conductivity bubbles must be included and the transconductivity cannot be written as a product of the impurity-averaged conductivities of the two subsystems. See also Ref. 19.

[17] It is easy to verify (15) independently by the following simple argument, which takes into account the external field experienced by layer 2 due to charge perturbations in layer 1:

$$\begin{aligned}(-e)\ j_2^\alpha(\boldsymbol{q},\omega) &= \sum_\delta\sigma_{22}^{\alpha\delta}(\boldsymbol{q},\omega)E_2^\delta(\boldsymbol{q},\omega) \\ &= \sum_\delta\frac{\boldsymbol{q}^\delta}{i}\sigma_{22}^{\alpha\delta}(\boldsymbol{q},\omega)\frac{1}{(-e)}V_{12}(\boldsymbol{q},\omega)\rho_1(\boldsymbol{q},\omega) \\ &= \sum_{\gamma,\delta}\frac{\boldsymbol{q}^\delta}{-ie}\sigma_{22}^{\alpha\delta}(\boldsymbol{q},\omega)V_{12}(\boldsymbol{q},\omega)\frac{\boldsymbol{q}^\gamma}{\omega}j_1^\gamma(\boldsymbol{q},\omega) \\ &= \sum_{\beta,\gamma,\delta}\left[\frac{q^\delta q^\gamma}{ie^2\omega}\sigma_{22}^{\alpha\delta}(\boldsymbol{q},\omega)V_{12}(\boldsymbol{q},\omega)\sigma_{11}^{\gamma\beta}(\boldsymbol{q},\omega)\right]E_{1\text{ext}}^\beta(\boldsymbol{q},\omega),\end{aligned}$$

where we used continuity equation to relate ρ_1 and j_1. The charge of the carriers was taken to be $-e$, although a generalization to mixed carrier systems is straightforward. The term in the square brackets is the transconductivity tensor, which agrees with Eq. (15).

[18] B. Laikhtman and P. M. Solomon, Phys. Rev. B **41**, 9921 (1990); P. M. Solomon and B. Laikhtman, Superlatt. Microstruct. **10**, 89 (1991).

[19] This factorization is not possible if one must consider scattering processes where the electrons in the two quantum wells scatter against the *same* impurities. The main source for impurity scattering is due to the ionized impurities in the *outside* barriers and hence the electrons in a given well feel mainly their "own" impurities. The ratio of the strength of the screened charged impurity potential $V_{\mathrm{imp},i}(q)$ in identical wells separated by a distance d, with well 1 closer to the impurity than well 2, is (within the Thomas-Fermi screening approximation) $V_{\mathrm{imp},2}(q)/V_{\mathrm{imp},1}(q) = q\exp(-qd)/[q_{\mathrm{TF}}(1-e^{-2qd})+q]$, independent of the distance of the impurities to the wells. For experimental parameters in Ref. 1, this ratio is $\lesssim 0.05$. Further, the barrier separating the two quantum wells is undoped (and consequently has a low impurity concentration) and hence we feel that these correlated impurity processes can safely be neglected.

[20] One should note that Fig. 3 does not include all possible diagrams. Examples of such higher-order diagrams are analyzed in Sec. III D.

[21] See, for example, Ref. 15, Sec. 7.1.c.

[22] B. L. Al'tshuler and A. G. Aronov, Zh. Eksp. Teor. Fiz. **77**, 2028 (1979) [Sov. Phys. JETP **50**, 968 (1979)].

[23] P. A. Lee and T. V. Ramakrishnan, Rev. Mod. Phys. **57**, 287 (1985).

[24] J. Rammer and H. Smith, Rev. Mod. Phys. **58**, 323 (1986).

[25] M. Bønsager, K. Flensberg, B. Y.-K. Hu, and A.-P. Jauho (unpublished).

[26] B. L. Altshuler, D. Khmel'nitskii, A. I. Larkin, and P. A. Lee, Phys. Rev. B **22**, 5142 (1980).

[27] A. Kamanev and Y. Oreg, Phys. Rev. B **52**, 7516 (1995).

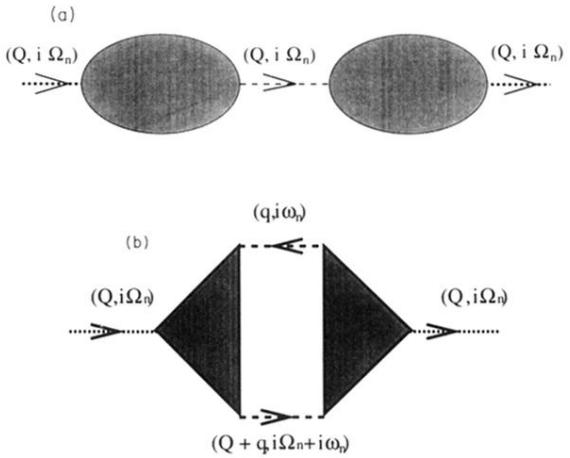

FIG. 1. Diagrams corresponding to the current-current correlation function to (a) first and (b) second order in the interlayer Coulomb interaction. The shaded triangles correspond to the Δ's given in Eqs. (17) and (18), the dashed lines to the interaction, the dotted lines to the external current operators, and the arrowheads to the direction of momentum and energy transfer.

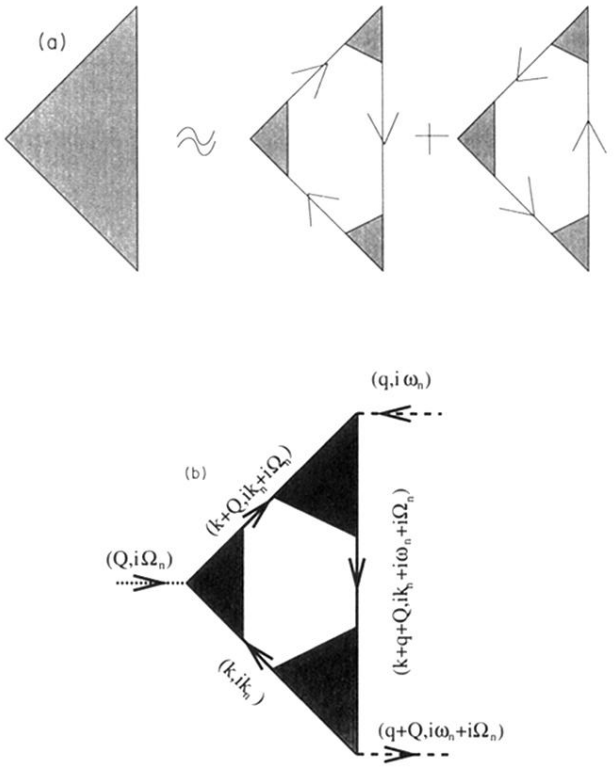

FIG. 3. Function Δ for the case in which vertex corrections are included at each of the individual charge and current vertices. (a) shows the decomposition of Δ into diagrams with clockwise- and counterclockwise-moving Green functions, with the gray shaded areas indicating vertex corrections. (b) shows one of these diagrams in greater detail. Here $k^{\alpha}\gamma$ is the current vertex, the Γ is the charge vertex, the dashed line is incoming momentum and frequency, the dotted lines are the interaction $V_{12}(q,\omega)$, and the solid lines with arrows are the Green function. Normal momentum and energy conservation rules apply at the vertices.